

Full correlation single-particle positron potentials for a positron and a positronium interacting with atoms

A. Zubiaga* and F. Tuomisto

*Department of Applied Physics, Aalto University,
P.O. Box 14100, FIN-00076 Aalto Espoo, Finland*

M. J. Puska

*COMP, Department of Applied Physics, Aalto University,
P.O. Box 11100, FIN-00076 Aalto Espoo, Finland*

Abstract

In this work we define single-particle potentials for a positron and a positronium atom interacting with light atoms (H, He, Li and Be) by inverting a single-particle Schrödinger equation. For this purpose, we use accurate energies and positron densities obtained from the many-body wavefunction of the corresponding positronic systems. The introduced potentials describe the exact correlations for the calculated systems including the formation of a positronium atom. We show that the scattering lengths and the low-energy *s*-wave phase shifts from accurate many-body calculations are well accounted for by the introduced potential. We also calculate self-consistent two-component density-functional theory positron potentials and densities for the bound positronic systems. They are in a very good agreement with the many-body results, provided that the finite-positron-density electron-positron correlation potential is used, and they can also describe systems comprising a positronium atom. We argue that the introduced single-particle positron potentials defined for single molecules are transferable to the condensed phase when the inter-molecular interactions are weak. When this condition is fulfilled, the total positron potential can be constructed in a good approximation as the superposition of the molecular potentials. Finally we address other concerns regarding the distinguishability of the positronium complex and the role of the accompanying electron in the positronium atom.

* asier.zubiaga@aalto.fi

I. INTRODUCTION

Although the chemistry of the positron in crystalline solids and soft-condensed matter has an intrinsic interest by itself, it is mainly studied in connection of probing the electron chemistry and the open volume of materials by positrons. Thermalized positrons become localized inside open volume defects such as vacancies and voids where the repulsion by the nucleus is minimum. When probing soft matter, the positron chemistry has to be taken into account because a positron can bind an electron and form a positronium (Ps) atom before getting trapped into open volume pockets [1]. The annihilation properties of the positron are determined by the local electronic structures and the distribution of the open volume. The positron annihilation spectroscopy (PAS) exploits this property to measure the type and concentration of vacancies in metals and semiconductors [2]. By measuring the lifetime of Ps, the distribution of open volume has been studied in porous SiO₂ [3, 4], polymers [5] and biostructures [6].

The interpretation of PAS experiments benefits from the comparison to computational predictions. However, the description of an electron-positron system embedded in a host material requires addressing the correlations of light particles beyond the adiabatic approximation, the quantum-mechanical delocalization and the zero-point energy. Regrettably, using many-body techniques for a full quantum-mechanical treatment of the problem is clearly beyond the present-day computational capacity. Instead, in metals and semiconductors the distributions and the annihilation properties of positrons can be calculated from first principles to a good accuracy within the two-component density functional theory (2C-DFT) and the local density approximation (LDA) for the exchange and correlation functionals [7]. For a delocalized positron in a perfect lattice the scheme works specially well because the electron-positron correlation energy functional is known very accurately within the LDA in this limit. Moreover, the same method can be applied also for positrons trapped at vacancies. The calculated positron annihilation parameters can then be used for a quantitative analysis of the experimental results for metals and semiconductors. However, the 2C-DFT scheme is considered to be unable to describe Ps and instead semiempirical methods have been employed to describe the matter-Ps interaction [8–10].

The many-body wavefunctions of small positronic systems composed by a positron interacting with a light atom or a small molecule can be calculated to a good accuracy using the

Quantum Monte-Carlo (QMC) [11–16] and Configuration Interaction (CI) [17] methods. In this work, we have obtained accurate positron energies and densities for positronic atoms including a positron (e^+H , e^+He , e^+Li and e^+Be) and Ps (HPs and LiPs) by an exact diagonalization stochastic variational method (SVM) using an explicitly correlated Gaussian (ECG) function basis set.

In e^+Li an electron from Li forms a Ps atom with the positron and becomes bound to the Li^+ ion. In e^+Be the polarized electron cloud binds the positron. In HPs and LiPs the unpaired atom electrons form a chemical bond that binds the Ps strongly to the atom. On the other hand, the positron is not bound to the atom in the e^+H and e^+He systems. ECG-SVM accounts for more correlation energy for the bound states [18–20] and the resulting binding energies are larger than for QMC and CI.

On the basis of our many-body results we propose a single-particle potential for the positron and we derive it for all the positronic systems by inverting a single-particle Schrödinger equation. We check their accuracy by comparing the ensuing scattering lengths and the s-wave phase shifts to the corresponding many-body values. We also compare the many-body densities and the introduced single-particle potentials to the corresponding 2C-DFT results for bound e^+Li , e^+Be , HPs and LiPs. The agreement seen predicts that 2C-DFT can be the starting point to describe positron bound states including systems in which Ps is formed. Finally, we discuss the utility of the single-particle effective potentials to approach a practical and predictive description of positron and Ps states in condensed matter.

The organization of the present paper is as follows. The many-body ECG-SVM as well as the 2C-DFT schemes are shortly described in Chapter II. Chapter III presents and discusses the effective single-particle potentials, the elastic scattering parameters and the self-consistent 2C-DFT results. Chapter IV is devoted to discuss the utility of the introduced potentials to describe positron and Ps states in condensed matter and chapter V presents our conclusions.

II. COMPUTATIONAL METHODS

A. ECG-SVM

ECG-SVM [21] is an all-particle quantum ab-initio method used to calculate the many-body wavefunction of N particles (electrons, positrons and nuclei) interacting through the Coulomb interaction. The Hamiltonian of the system with the kinetic energy of the center-of-mass (CM) subtracted is

$$H = \sum_i \frac{p_i^2}{2m_i} - T_{CM} + \sum_{i<j} \frac{q_i q_j}{4\pi\epsilon_0 r_{ij}}, \quad (1)$$

where \vec{p}_i is the momentum, m_i the mass, and q_i the charge of the i^{th} particle, r_{ij} is the distance between the i^{th} and j^{th} particles and T_{CM} the kinetic energy of the CM. The hadronic nucleus is treated as a point particle without structure, on equal footing with the electrons and the positron. The wavefunction is expanded in terms of a linear combination of properly antisymmetrized ECG functions,

$$\Psi(x) = \sum_{i=1}^s c_i \mathcal{A} \left[\exp^{-\frac{1}{2}x A^i x} \right] \otimes \chi_{SMs}, \quad (2)$$

where A^i are the non-linear coefficient matrices and c_i the mixing coefficients of the eigenvectors. The antisymmetrization operator \mathcal{A} acts on the indistinguishable particles and χ_{SMs} is a spin eigenfunction with $\hat{S}^2 \chi_{SMs} = S(S+1)\hbar^2 \chi_{SMs}$ and $\hat{S}_z \chi_{SMs} = M_S \hbar \chi_{SMs}$. The ECG basis uses Jacobi coordinate sets $\{x_1, \dots, x_{N-1}\}$ with the reduced mass $\mu_i = m_{i+1} \sum_{j=1}^i m_j / \sum_{j=1}^{i+1} m_j$ that allows for a straightforward separation of the CM movement. All the systems we have considered so far have zero total angular momentum, so we do not need to include spherical harmonics to describe the orbital motion. The electron density is $n_-(r) = \sum_{i=1}^{N_e} \langle \Psi | \delta(\vec{r}_i - \vec{r}_N - \vec{r}) | \Psi \rangle$ and the positron density is $n_+(r) = \langle \Psi | \delta(\vec{r}_p - \vec{r}_N - \vec{r}) | \Psi \rangle$, where \vec{r}_i , \vec{r}_p , and \vec{r}_N are the coordinates of the i^{th} electron, the positron and the nucleus, respectively.

The ECG basis sets used in this work comprise between 200 and 2000 functions. Typically, systems with more particles need larger function basis sets for an accurate determination of the wavefunction. The non-linear coefficients $A_{\mu\nu}^i$ are to be optimized to avoid very large basis sets. SVM, which is better suited for functions with a large number of parameters than direct search methods, is used for this purpose. The values of the parameters are varied randomly and the new values are kept only if the update lowers the total energy of

the system. The success of the ECG-SVM method relies on the efficient calculation of the matrix elements.

Bound e^+Li , e^+Be , and LiPs have all relatively large extent but e^+Be converges noticeably slower. We obtain 2.33×10^{-3} au for the positron binding energy in e^+Be , while the most accurate value from the literature is 3.163×10^{-3} au [19]. On the other hand, the dissociation energy of e^+Li against Li^+ and Ps, 2.42×10^{-3} au, and the Ps binding energy of LiPs, 11.011×10^{-3} au, are closer to the ECG-SVM reference values, 2.4821×10^{-3} au [18] and 12.371×10^{-3} au [19], respectively. Finally, we obtain 39.187×10^{-3} au for the Ps binding energy in HPs, in excellent agreement with the reference value of 39.19×10^{-3} au [20].

Unbound e^+H and e^+He can be calculated variationally adding an external confining potential. We have used a weak two-body attractive potential,

$$V(r_p) = \begin{cases} 0 & , \quad r < R_0 \\ \alpha(r_p - R_0)^2 & , \quad r \geq R_0, \end{cases} \quad (3)$$

binding the positron to the hadronic nucleus in a similar fashion to the confinement potential used by Mitroy et al. to describe positrons scattering off atoms [22]. The potential is different from zero only when the nucleus-positron distance r_p grows above the boundary value R_0 , and then it has a parabolic increase. R_0 and α were set so that the average nucleus positron distance $\langle r_p \rangle \gtrsim 50$ au. The confinement radius is chosen large enough (100 au) so that the shape of the wavefunction is not affected by the confinement potential in the interaction region of the positron or Ps with the atom. The resulting $\langle r_p \rangle$ is large and the interaction energy is small.

For unbound e^+H and e^+He the asymptotic state of the interacting system, when the positron is far from the atom, is the main scattering channel, i.e., the positron scatters off the neutral atom, and for bound systems the main scattering channel is the main dissociation channel. e^+Be splits into a neutral atom and a positron, e^+Li splits into a Li^+ ion and a Ps atom and both HPs and LiPs dissociate into neutral atoms and Ps. We define the positron interaction energy as $E_{int}^{e^+} = E_{e^+X} - E_X$, i.e., the difference between the energy of the interacting positronic system, E_{e^+X} , and the atom without the positron, E_X . The Ps interaction energy, $E_{int}^{Ps} = E_{e^+X/XP_s} - E_{X^+/X} - E_{Ps}$ is the difference between the energy of the interacting system, E_{e^+X/XP_s} , and the sum of the total energies of the positive ion or the atom, $E_{X^+/X}$, and Ps, E_{Ps} , after Ps has dissociated.

Table I. Main properties of the calculated systems. The first four columns give the name of the system, the size of the basis used, the total energy, and the mean positron-nucleus distance $\langle r_p \rangle$. The next three columns give the asymptotic state, the total energy of the corresponding atom or ion and the interaction energy.

System	Basis size	Energy (au)	$\langle r_p \rangle$ (au)	Asymptotic state	Atom/Ion Energy (au)	$E_{int}^{e^+}/E_{int}^{Ps}$ (au)
e ⁺ H	200	-0.49974	67.47	e ⁺	-0.5 (H)	0.262×10^{-3}
e ⁺ He	1000	-2.90332	56.98	e ⁺	-2.9036937 (He)	0.372×10^{-3}
e ⁺ Be	2000	-14.6694	10.972	e ⁺	-14.6670283 (Be) -14.3246131 (Be ⁺)	-2.33×10^{-3}
e ⁺ Li	1000	-7.53226	9.928	Ps	-7.2798377 (Li ⁺)	-2.42×10^{-3}
HPs	1000	-0.78919	3.662	Ps	-0.25 (Ps)	-39.187×10^{-3}
LiPs	2000	-7.73898	6.432	Ps	-7.4779733 (Li)	-11.011×10^{-3}

B. Two-component DFT

Within the LDA of the 2C-DFT the total energy functional of a positronic atom is

$$E[n_-(r), n_+(r)] = F_1[n_-] + F_2[n_+] + E_C^{ep}[n_-, n_+] + E_{corr}^{ep}[n_-, n_+], \quad (4)$$

where $E_C^{ep}[n_-, n_+]$ is the attractive Coulomb interaction between the electrons and the positron and $E_{corr}^{ep}[n_-, n_+]$ is the electron-positron correlation energy functional. $F_1[n]$ is the usual one-component density functional

$$F_1[n] = E_{kin}[n] + E_{ext}[n] + E_H[n] + E_{xc}[n], \quad (5)$$

where $E_{kin}[n]$ is the Kohn-Sham kinetic energy and $E_{ext}[n]$, $E_H[n]$, and $E_{xc}[n]$ are the electron(positron)-nucleus interaction, the Hartree energy functional and the exchange-correlation energy functional, respectively. For the last one, we have used the parametrization by Perdew and Zunger [23]. The self-interaction corrected (SIC) density functional for a single positron $F_2[n]$ is

$$F_2[n] = E_{kin}[n] + E_{ext}[n]. \quad (6)$$

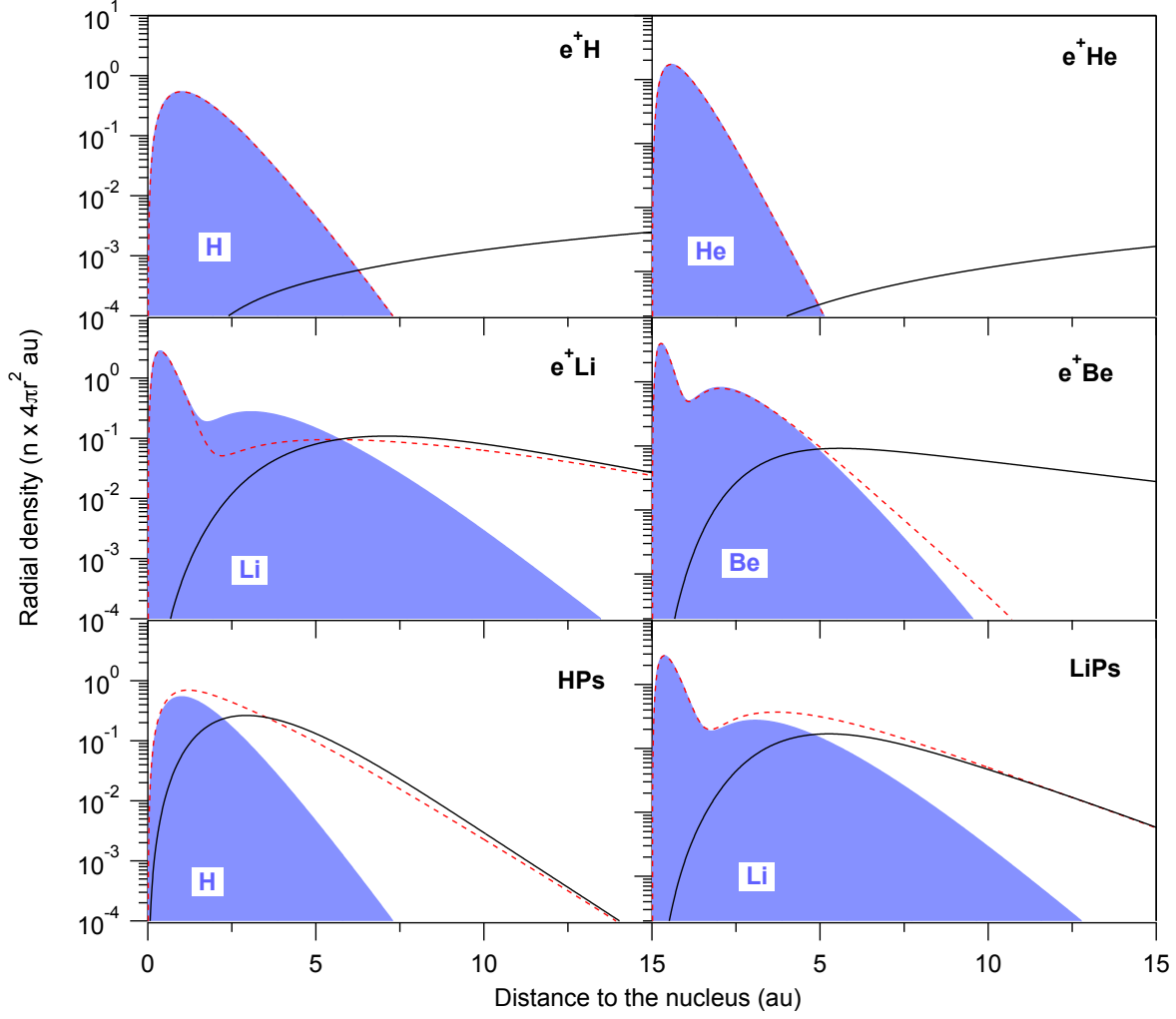


Figure 1. (Color online) Electron and positron densities of the calculated systems. The electron densities of the isolated atoms (filled blue curves), and the interacting positron-atom systems (red broken curves), as well as the positron densities (black full curves) are given.

The asymmetric treatment of the electron and positron self-interactions for positron states in solids has been shown to give results in a quantitative agreement with experiments [24, 25].

The resulting Kohn-Sham equations for the electron ϕ_i^- and positron ϕ_i^+ orbitals are

$$\left[-\frac{\nabla^2}{2} - \frac{Z}{r} + \int \frac{n_-(x) - n_+(x)}{|\vec{r} - \vec{x}|} d\vec{x} + \frac{\delta E_{xc}[n_-]}{\delta n_-} + \frac{\delta E_{corr}^{ep}[n_+, n_-]}{\delta n_-} \right] \phi_i^- = \epsilon_i^- \phi_i^- \quad (7)$$

$$\left[-\frac{\nabla^2}{2} + \frac{Z}{r} - \int \frac{n_-(x)}{|\vec{r}-\vec{x}|} d\vec{x} + \frac{\delta E_{corr}^{ep}[n_+, n_-]}{\delta n_+} \right] \phi^+ = \epsilon^+ \phi^+, \quad (8)$$

where Z is the atomic number of the nucleus and ϵ_i^- and ϵ^+ are the electron and positron energy eigenvalues, respectively. Equations 7 and 8 are solved self-consistently with a DFT code that solves the all-electron and positron radial Kohn-Sham equations [26]. The Coulomb potential plotted in figure 2 is composed by the second and third terms of equation 8.

In our 2C-DFT energy functional we use a two-component electron-positron correlation energy functional $E_{ep}[n_+, n_-]$. To build up this functional, there is only data for a homogeneous electron-positron plasma in the metallic regime calculated by Lantto [27]. The LDA parametrization of reference [25] describes correctly $E_{ep}[n_+, n_-]$ and $V_{ep}[n_+, n_-] = \delta E_{ep}[n_+, n_-] / \delta n_+$ for the electron densities typical in metals and semiconductors $r_s = (3/4/\pi/n)^{1/3} \sim 3$ au. We have extrapolated the functional for lower densities using that $E_{ep}[n_+, n_-]$ is symmetric in n_+ and n_- and at the limit of the vanishing positron density ($r_s \sim 20$ au) the energy of a single positron in a homogeneous electron gas should be obtained [28, 29]. We also impose that the energy functional is smooth and it has a smooth derivative everywhere. Finally we set a cut-off in $V_{ep}[n_+, n_-]$ when the r_s parameter of the electrons and the positron are larger than 20 au.

III. RESULTS

The ionization energies of H and He are 0.5 au and 0.90369 au, respectively. They are well above the binding energy of Ps (0.25 au), therefore the electrons, as shown in figure 1, remain tightly bound to the nuclei without an appreciable polarization. The positron is completely delocalized in these systems. The ionization energy, 0.34242 au, of the closed 2s orbital of Be is only slightly larger than the Ps binding energy so that the atom becomes polarized and the positron is bound by the induced dipole. On the other hand, the Li ionization energy of 0.198 au is lower than the binding energy of Ps and the positron forms a Ps cluster with the Li 2s electron [30]. In HPs and LiPs, the electron in Ps forms a strong chemical bond with the unpaired s electron of the atom, keeping Ps as a distinguishable unit.

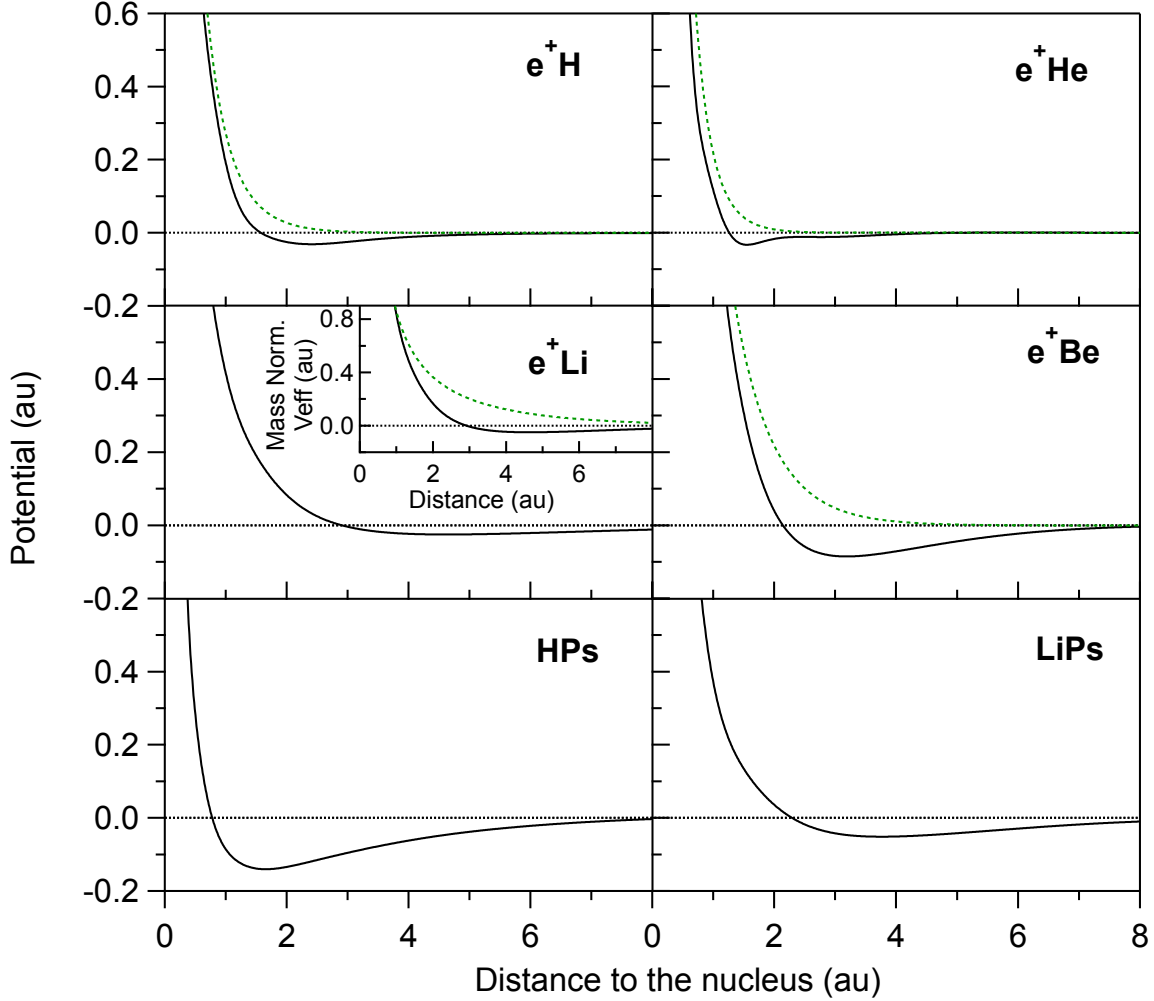


Figure 2. (Color online) V_{eff} (black curves) of all the calculated systems and the Coulomb potentials (green dotted curves) of the systems composed by an atom and a positron. For e^+Li , HPs and LiPs the Ps V_{eff} have been plotted. The inset in the e^+Li panel compares the mass normalized V_{eff} and the Coulomb potentials.

A. Effective potentials

We introduce now an effective single-particle potential V_{eff} using our many-body results and in Chapter IV we will propose it as the starting point to describe positron and Ps states in condensed matter. We invert a single-particle Schrödinger equation using the positron

densities of the interacting systems and obtain

$$V_{eff}(r) = E_{eff} + \frac{1}{2M_{eff}} \frac{\nabla^2 \sqrt{n_+(r)}}{\sqrt{n_+(r)}}. \quad (9)$$

The effective energy E_{eff} is the interaction energy of the asymptotic state in table I. For e^+Li , HPs and LiPs the effective mass M_{eff} is the mass of Ps ($2m_e$) and for the other systems it is the mass of the positron (m_e). The effective potential is a single-particle potential for the positron even in systems where Ps is formed. We remark that the effective potential describes a system comprising a Ps atom by naming it as the Ps effective potential.

We also define a single-particle mass-normalized Ps effective potential $V_{eff}^{Ps} = 2E_{int}^{Ps} + \nabla^2(\sqrt{n_+})/(2\sqrt{n_+})$ with the effective mass m_e . The densities obtained by solving the Schrödinger equation with the mass-normalized potential are the same as those of V_{eff} and the energies are multiplied by a factor of 2. In the present work, we use the mass-normalized potential to compare the Ps V_{eff} to the corresponding positron DFT potential.

According to figure 2, when $r \lesssim 1$ au the positron-nucleus Coulomb repulsion dominates over the electron-positron attractive Coulomb and correlation potentials. V_{eff} becomes attractive at larger separations, when the electron-positron correlation is comparable to the Coulomb repulsion. The repulsive core of V_{eff} range from $r \lesssim 1.2$ au for e^+H and e^+He and $r \lesssim 2-3$ au for e^+Li and e^+Be . Although the attractive V_{eff} well is slightly deeper for e^+H than for e^+He , due to the larger polarizability of H, they are very shallow for both unbound systems. For bound e^+Be the minimum of V_{eff} is deeper, -84.58×10^{-3} au at $r=3.18$ au. The minimum value of the Ps V_{eff} potential of e^+Li is shallower, -24.57×10^{-3} au at $r=4.62$ au, but it extends until longer distances. Finally, the attractive Ps V_{eff} wells of the strongly bound HPs and LiPs are deep, -0.280 au and -0.102 au, respectively.

To show that V_{eff} can predict the correct positron density and interaction energy, we have calculated the positron (Ps) binding energy to Be (Li^+) by solving numerically the radial single-particle Schrödinger equation. For the ground state it reduces to the one-dimension problem

$$-\frac{1}{2M_{eff}} \frac{d^2U}{dr^2} + V_{eff}U = EU, \quad (10)$$

where $U = r\Psi$ and Ψ is the s-type wavefunction. The boundary conditions for U are $U(r=0)=0$ and $U(r \rightarrow \infty)=0$. For e^+Li , HPs and LiPs the effective potentials are the Ps V_{eff} potentials and $M_{eff}=2m_e$. The resulting binding energy and $\langle r_p \rangle$ given by equation 10 are, $E_b = 2.414 \times 10^{-3}$ au and $\langle r_p \rangle = 10.213$ au for e^+Li , $E_b = 2.33 \times 10^{-3}$ au and $\langle r_p \rangle =$

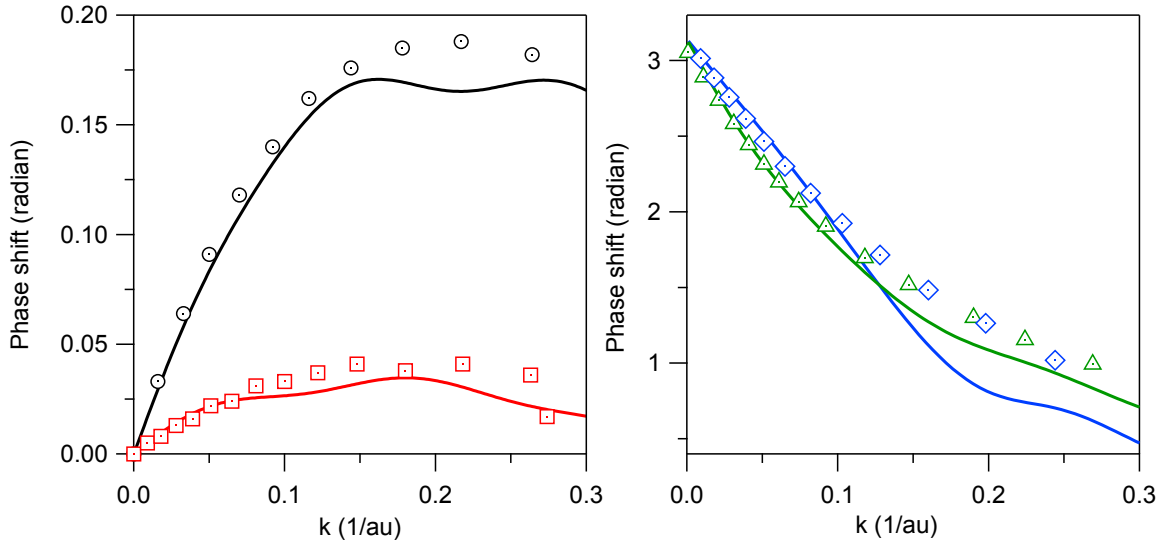


Figure 3. (Color online) s-wave phase shifts for positrons scattering off H (black curve), He (red curve), Li (blue curve) and Be (green curve). The many-body values obtained by Zhang et al. [31] for H (black circles), He (red squares) and Li (blue diamonds) and Bromley et al. [33] for Be (green triangles) are also shown.

11.104 au for e^+Be , $E_b=39.210\times 10^{-3}$ au and $\langle r_p \rangle = 3.673$ au for HPs, and $E_b = 10.394$ au and $\langle r_p \rangle = 6.457$ au for LiPs.

B. Scattering Lengths

In order to study the adequacy of V_{eff} to model positron and Ps states, we consider a positron or Ps scattering off light atoms. Many-body calculations of the s-wave phase shifts (δ_0) and scattering lengths (a_0) exist for e^+H , e^+He , e^+Li and e^+Be . Zhang et al. [31] used the stabilized ECG-SVM to calculate the positron a_0 of H and He and the Ps a_0 of Li^+ . Houston et al. [32] applied Hylleraas wavefunctions and the Kohn variational method to positrons scattering off H and Bromley et al. [33] studied positron scattering off Be using polarized orbital wavefunctions.

Here we calculate δ_0 and a_0 using the corresponding V_{eff} or Ps V_{eff} and compare them to the many-body values of the literature. For a positron scattering off Li, the polarization of the target atom and the formation of Ps are important already at low energies [34, 35] and

therefore the Ps V_{eff} values of e^+Li are compared to the many-body Ps a_0 and δ_0 of Li^+ . We obtain the s-wave scattering wavefunction for a positron with the energy $E = k^2/2M_{eff}$ by solving equation 10. At large distances from the nucleus the wavefunction has the form

$$\lim_{r \rightarrow \infty} \psi_0 = \frac{\sin(kr + \delta_0)}{kr}. \quad (11)$$

The wavefunction calculated numerically is fitted to this asymptote to obtain δ_0 as a function of k . a_0 is then calculated at the low-energy limit from $k \cot \delta_0 = -1/a_0 + O(k^2)$.

Table II. Positron (e^+H , e^+He and e^+Be) and Ps (e^+Li) scattering lengths. The first column shows the values computed using V_{eff} and the last column are many-body calculations from the literature. All the values are given in au.

e^+H	-1.86	-2.094 [31], -2.10278 [32]
e^+He	-0.55	-0.474 [31]
e^+Be	18.76	16 [33]
Ps- Li^+	12.19	12.9 [31]

The calculated $\delta_0(k)$ are plotted in figure 3. They show a good agreement with the many-body values for $k \lesssim 0.1 \text{ au}^{-1}$ which suggests that (Ps) V_{eff} will remain valid to describe quasi-thermalized positrons at room temperature. For larger momenta the dynamical correlation becomes important and our values are systematically slightly lower. For Ps scattering off Li^+ the difference is the largest, 0.3-0.4 radians, because both the target and the projectile are deformed. For a positron scattering off Be the agreement is very good, considering that the positron binding energy to Be is 0.8×10^{-3} au smaller (26%) than the best many-body value [19] and 0.5×10^{-3} au smaller (16%) than the binding energy by Bromley et al. [33] However the a_0 value shows the largest mismatch with the reference many-body value. For H, He and Li the present a_0 are comparable to the many-body values.

C. Two-component DFT

2C-DFT is the basis of efficient predictive modeling of positron states in condensed matter. In this section, we study to which extent 2C-DFT is able to describe the bound

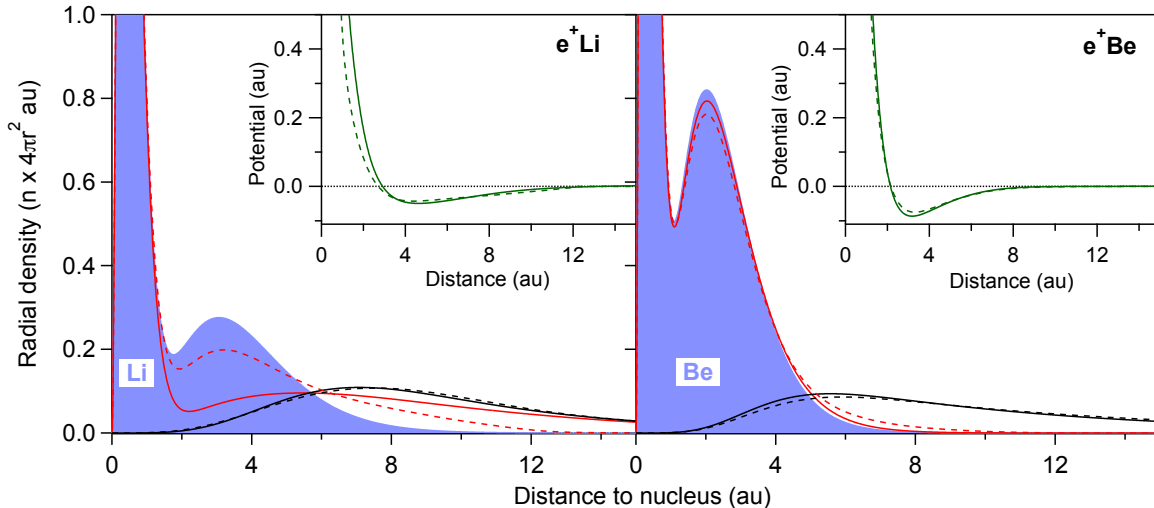


Figure 4. (Color online) ECG-SVM (full curves) and 2C-DFT (broken curves) densities and positron potentials for $e^+\text{Li}$ and $e^+\text{Be}$. The radial electron densities of the isolated atoms (filled blue curves), and the interacting positron-atom systems (red curves), as well as the positron densities (black curves) are represented in the main panel. The insets compare the single-particle positron potentials. For $e^+\text{Li}$ the mass normalized potential has been plotted.

states of positrons and Ps interacting with an atom. The analysis of $e^+\text{Li}$, HPs, and LiPs allows us to draw conclusions also about systems including a Ps cluster. Using the vanishing positron-density limit for the electron-positron correlation energy and potential [28, 29] the LDA 2C-DFT doesn't predict the binding of positrons to atoms. We use instead $E_{ep}[n_+, n_-]$, a LDA functional which depends on the electron and positron densities and it predicts the formation of bound atom-positron states.

Overall, the 2C-DFT predicts accurate positron densities and potentials comparable to the many-body results. Figure 4 compares the radial electron and positron densities of $e^+\text{Li}$ and $e^+\text{Be}$ calculated with 2C-DFT and ECG-SVM. The 2C-DFT positron density of $e^+\text{Be}$ matches the many-body density whereas the 2C-DFT electron density is slightly more delocalized than the many-body density. The 2C-DFT positron density of $e^+\text{Li}$ is also accurate, however, within 2C-DFT the electrons are more tightly bound to the nucleus than in the many-body calculation. The potential wells of the 2C-DFT positron potentials match V_{eff} of $e^+\text{Be}$ and the mass-normalized V_{eff}^{Ps} of $e^+\text{Li}$. Close to the Li nucleus the 2C-DFT positron potential is less repulsive than V_{eff} but the effect on the positron density is minor.

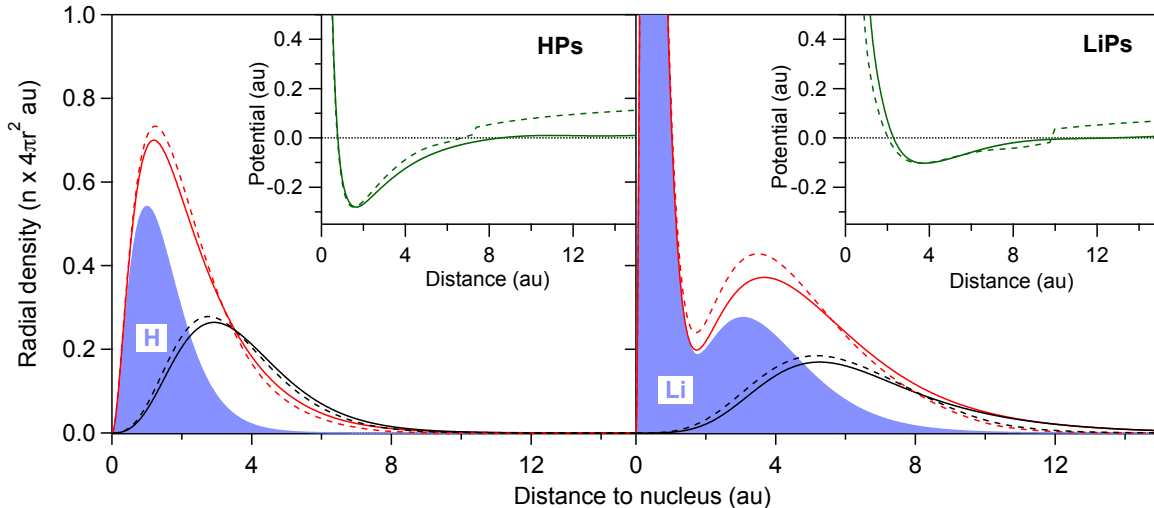


Figure 5. (Color online) ECG-SVM (full curves) and 2C-DFT (broken curves) densities and potentials for HPs and LiPs. The radial electron densities of the isolated atoms (filled blue curves), and the interacting positron-atom systems (red curves), as well as the positron densities (black curves) are represented in the main panels. The insets compare the 2C-DFT positron potential and the ECG mass normalized potential V_{eff}^{Ps} . The 2C-DFT potentials have been shifted upward to match the minima of the ECG potentials.

Figure 5 shows that the 2C-DFT potential of HPs decays to zero faster than V_{eff} , resulting in a more localized positron density. The 2C-DFT positron density is slightly more localized for LiPs also because the 2C-DFT potential is less repulsive close to the nucleus. The 2C-DFT electron densities are also more localized than the corresponding many-body densities, specially for LiPs, and they pull the positron inwards. The 2C-DFT positron potentials show a kink caused by the cut-off imposed to the potential when the densities are low. Without the cut-off the potentials have a long-range attractive tail which makes the positron densities too delocalized. Many-body calculations at the low-density range of the electron-positron plasma would be required to obtain an electron-positron correlation potential which is accurate beyond the metallic regime of densities.

The asymmetric behavior of the 2C-DFT electron and positron densities with respect to the many-body calculations reflects the means of DFT to describe correlations in the interacting many-body system [36]. The electron self-interaction causes the 2s orbital of e^+Li to be poorly described in DFT. Moreover, 2C-DFT within LDA cannot describe ac-

curately strongly-correlated systems like Ps. Accordingly, the 2C-DFT densities of e^+Li don't show the formation of Ps. However, in HPs and LiPs at long separations the electron and positron densities converge as expected when Ps forms. Overall, figures 4 and 5 show convincingly that the electron-positron correlation potential derived from the energy of an electron-positron plasma yields surprisingly accurate positron densities in bound positronic atoms, including systems where Ps forms.

The positron binding energies of all the studied systems are only qualitative, reflecting the general inadequacy of LDA to accurately describe binding between atoms. Moreover, it is a well known problem that DFT within LDA is not able to describe dispersion interactions [37].

IV. V_{eff} FOR POSITRON AND Ps STATES IN CONDENSED MATTER

It is well established that the 2C-DFT yields reliable densities for positrons trapped at vacancies inside metals and semiconductors [25]. To simplify the calculations or to compare different approaches, it would be desirable to calculate the positron potentials also as superpositions of atomic or molecular V_{eff} in condensed matter. However, the transferability of V_{eff} deduced from single positronic atoms or molecules is of concern. The trapping of positrons in vacancies inside metals and semiconductors occurs partly because the valence electrons relax into the vacancy as attracted by the positron increasing the binding energy and the degree of localization of the positron. In the 2C-DFT this is taken into account through the electron-positron correlation functional which lowers the energy of the positron inside the vacancy. However, in V_{eff} obtained from an atom-positron system the valence electrons remain bound to the atom and its atomic superposition cannot predict the positron trapping inside vacancies of crystalline solids. The utility of V_{eff} will not be limited by this problem in condensed matter systems where the electronic structures of the constituent atoms or molecules remain nearly undisturbed like in molecular soft condensed matter and liquids where inter-molecular interactions are weak.

The superposition of molecular V_{eff} potentials is specially interesting to study Ps embedded in molecular materials like polymers, liquids or biostructures. Typically, the exchange repulsion between the Ps and the HOMO-LUMO gap (~ 0.5 au) of closed shell molecules prevents the formation of a Ps bound state. Instead Ps is localized in open volume pockets at the potential wells induced by the surrounding molecules. The applicability of the

proposed scheme in atomic models of the material requires that V_{eff} can be derived for the molecules forming the material. The calculation of V_{eff} requires high quality many-body positron densities what is computationally demanding with the present computing capacity. Smaller systems like HePs can be studied [38, 39], instead. He does not bind Ps due to its closed shell structure and its low polarizability. It possesses a HOMO-LUMO gap in a spin-compensated electron structure similarly to molecular matter and thus it provides a good model system to study the interaction of Ps. The knowledge gained studying model systems would allow building V_{eff} when ab-initio methods cannot be used. Moreover, our notion that the computationally efficient 2C-DFT reproduces accurately the many-body single-particles potentials for systems with Ps, raises the expectation that it could be used to construct Ps V_{eff} .

V. CONCLUSIONS

We have calculated the ECG-SVM many-body wavefunctions for positronic systems including a light atom (H, He, Li and Be) and a positron or Ps. Based on these results we have proposed an effective single-particle positron potential by inverting the single-particle Schrödinger equation arising from the many-body positron density. V_{eff} is a single-particle potential for the positron interacting with an atom which includes the full many-body correlations and it also describes a positron inside a Ps atom. The many-body positron densities and binding energies are, by construction, predicted by the introduced potential. The scattering lengths are consistent with the many-body values of the literature and the s-wave phase shifts show also good agreement for moments $k \lesssim 0.1 \text{ au}^{-1}$. The low-energy correlations are well described by V_{eff} up to energies larger than that of quasi-thermalized positrons and Ps at room temperature. The success of V_{eff} to describe the positron when a Ps complex forms, suggests that the potential can be also a valid single-particle description for the low-energy (quasi-thermalized) positron forming Ps without solving the Schrödinger equation for the many-body system. This possibility should be further studied in connection with Ps interacting with molecular systems. The superposition of atomic or molecular V_{eff} to calculate the positron potentials and the ensuing positron distributions in molecular condensed matter can be a valid description of the positron in Ps when the inter-molecular interactions are weak and the transferability is not of concern.

We have also shown that the positron densities are well described within the 2C-DFT for bound e^+Li , e^+Be , HPs and LiPs when the finite positron-density functional is used for the electron-positron correlation energy. The self-consistent LDA 2C-DFT positron potentials reproduce the binding potential well of V_{eff} accurately and predict the many-body positron densities. Although 2C-DFT is less consistent predicting the electron densities, our results indicate that it yields good positron distributions also in the cases where Ps bound to atoms. This result opens the possibility to use 2C-DFT also to describe Ps interacting with extended systems.

ACKNOWLEDGMENTS

This work was supported by the Academy of Finland through the individual fellowships and the centre of excellence program. We acknowledge the computational resources provided by Aalto Science-IT project. Thanks are due to K. Varga for providing us the ECG-SVM code used in this work and to I. Makkonen for insightful discussions.

-
- [1] O. E. Mogensen, in *Positron Annihilation in Chemistry*, Springer Series in Chemical Physics, Vol. 58, edited by H. K. V. Lotsch (Springer-Verlag, 1995).
 - [2] F. Tuomisto and I. Makkonen, *Rev. Mod. Phys.* **85**, 1583 (2013).
 - [3] Y. Nagai, Y. Nagashima, and T. Hyodo, *Phys. Rev. B* **60**, 7677 (1999).
 - [4] L. Liskay, C. Corbel, P. Perez, P. Desgardin, M.-F. Barthe, T. Ohdaira, R. Suzuki, P. Crivelli, U. Gendotti, A. Rubbia, M. Etienne, and A. Walcarius, *Appl. Phys. Lett.* **92**, 063114 (2008).
 - [5] A. Uedono, R. Suzuki, T. Ohdaira, T. Uozumi, M. Ban, M. Kyoto, S. Tanigawa, and T. Mikado, *J. Polym. Sci. Part B* **36**, 2597 (1998).
 - [6] P. Sane, E. Salonen, E. Falck, J. Repakova, F. Tuomisto, J. Holopainen, and I. Vattulainen, *J. Phys. Chem. B letters* **113**, 1810 (2009).
 - [7] M. J. Puska and R. M. Nieminen, *Rev. Mod. Phys.* **66**, 841 (1994).
 - [8] S. J. Tao, *J. Chem. Phys.* **56**, 5499 (1972).
 - [9] M. Eldrup, D. Lightbody, and J. N. Sherwood, *Chem. Phys.* **63**, 51 (1981).
 - [10] H. Schmitz and F. Müller-Plathe, *J. Chem. Phys.* **112**, 1040 (2000).

- [11] Y. Kita, R. Maezono, M. Tachikawa, M. Towler, and R. J. Needs, *J. Chem. Phys.* **131**, 134310 (2009).
- [12] Y. Kita, R. Maezono, M. Tachikawa, M. Towler, and R. J. Needs, *J. Chem. Phys.* **135**, 054108 (2011).
- [13] D. Bressanini, M. Mella, and G. Morosi, *J. Chem. Phys.* **108**, 4756 (1997).
- [14] D. Bressanini, M. Mella, and G. Morosi, *J. Chem. Phys.* **109**, 1716 (1998).
- [15] D. Bressanini, M. Mella, and G. Morosi, *J. Chem. Phys.* **109**, 5931 (1998).
- [16] M. Mella, G. Morosi, D. Bressanini, and S. Elli, *J. Chem. Phys.* **113**, 6154 (2000).
- [17] R. J. Buenker and H. P. Liebermann, *J. Chem. Phys.* **131**, 114107 (2009).
- [18] J. Mitroy, *Phys. Rev. A* **70**, 024502 (2004).
- [19] J. Mitroy, *J. At. Mol. Sci.* **1**, 275 (2010).
- [20] S. Bubin and K. Varga, *Phys. Rev. A* **84**, 012509 (2011).
- [21] K. Varga and Y. Suzuki, *Phys. Rev. C* **52**, 2885 (1995).
- [22] J. Mitroy, J. Y. Zhang, and K. Varga, *Phys. Rev. Lett.* **101**, 123201 (2008).
- [23] J. P. Perdew and A. Zunger, *Phys. Rev. B* **23**, 5048 (1981).
- [24] E. Boroński and R. M. Nieminen, *Phys. Rev. B* **34**, 3820 (1986).
- [25] M. J. Puska, A. P. Seitsonen, and R. M. Nieminen, *Phys. Rev. B* **52**, 10947 (1995).
- [26] P. Giannozzi, S. Baroni, N. Bonini, M. Calandra, R. Car, C. Cavazzoni, D. Ceresoli, G. L. Chiarotti, M. Cococcioni, I. Dabo, A. Dal Corso, S. de Gironcoli, S. Fabris, G. Fratesi, R. Gebauer, U. Gerstmann, C. Gougoussis, A. Kokalj, M. Lazzeri, L. Martin-Samos, N. Marzari, F. Mauri, R. Mazzarello, S. Paolini, A. Pasquarello, L. Paulatto, C. Sbraccia, S. Scandolo, G. Sciauzero, A. P. Seitsonen, A. Smogunov, P. Umari, and R. M. Wentzcovitch, *Journal of Physics: Condensed Matter* **21**, 395502 (2009). We have modified the free-atom code included in the Quantum Espresso package for this calculations.
- [27] L. J. Lantto, *Phys. Rev. B* **36**, 5160 (1987).
- [28] J. Arponen and E. Pajanne, *Ann. Phys.* **121**, 343 (1978).
- [29] N. D. Drummond, P. L. Rios, R. J. Needs, and C. J. Pickard, *Phys. Rev. Lett.* **107**, 207402 (2011).
- [30] J. Mitroy, M. W. J. Bromley, and G. G. Ryzhikh, *J. Phys. B: At. Mol. Opt. Phys.* **35**, R81 (2002).
- [31] J. Y. Zhang and J. Mitroy, *Phys. Rev. A* **78**, 012703 (2008).

- [32] S. K. Houston and R. J. Drachman, *Phys. Rev. A* **3**, 1335 (1971).
- [33] M. W. J. Bromley, J. Mitroy, and G. G. Ryzhikh, *J. Phys. B: At. Mol. Opt. Phys.* **31**, 4449 (1998).
- [34] M. Basu and A. S. Gosh, *Phys. Rev. A* **43**, 4746 (1991).
- [35] M. R. McAlinden, A. A. Kernoghan, and H. R. J. Walters, *J. Phys. B: At. Mol. Opt. Phys.* **30**, 1543 (1997).
- [36] H. Saarikoski, A. Harju, M. J. Puska, and R. M. Nieminen, *Phys. Rev. Lett.* **93**, 116802 (2004).
- [37] E. R. Johnson, I. D. Mackie, and G. A. Dilabio, *J. Phys. Org. Chem.* **22**, 1127 (2009).
- [38] A. Zubiaga, F. Tuomisto, and M. J. Puska, *Phys. Rev. A* **85**, 052707 (2012).
- [39] A. Zubiaga and M. J. Puska, “Single particle effective potentials for Ps,” In preparation.